A 3D FINITE ELEMENT ANALYSIS OF STATIC STRESS CONCENTRATIONS AROUND A BROKEN FIBRE

Y. Swolfs[1*], L. Gorbatikh[1] and I.Verpoest[1]

[1]Department of Metallurgy and Materials Engineering, KU Leuven, Kasteelpark Arenberg 44, B-3001 LEUVEN (Belgium)
**Email address: yentl.swolfs@mtm.kuleuven.be*

Keywords:
Finite element analysis, stress concentrations, ineffective length, unidirectional composites

Abstract
All existing models for the stress redistribution after a single fibre breakage in a unidirectional fibre-reinforced composites use regular fibre packings. In the present work, the stress redistribution in random fibre packings was analyzed using three dimensional finite element analysis. Compared to regular fibre packings, random fibre packings result in a lower ineffective length and, when looking at fibres at the same distance from the broken fibre, in lower stress concentration factors and overload lengths. It was shown that an increase in fibre volume fraction has a similar effect as changing from regular to random fibre packings.

1 Introduction

The failure of the 0° continuous fibres in polymer composites generally coincides with the final failure of the composite. Hence, a profound understanding of the failure behaviour of 0° fibres is of utter importance. The most fundamental issue in strength models of unidirectional composites is the re-distribution of the axial stresses around a broken fibre. This results in stress concentrations on the fibres nearby the broken fibre. These stress concentrations increase the failure probability of the nearby fibres. It is quantified as the stress concentration factor (SCF), which is the ratio of the stress near the broken fibre over the stress far away from the fibre breakage [1].

The first models for SCFs were developed in the early seventies and are all shear lag models (SLM). These models assume that the matrix carries only shear loads and that the fibres carry all the axial loads. These assumptions enable an analytical solution for the SCFs. Unfortunately, SLMs are inaccurate when (1) the fibres are highly loaded, (2) the fibres have a high shear modulus, (3) the matrix has a high tensile stiffness or (4) the matrix yields. Moreover, SLMs for composites with random fibre spacing or with more than one type of fibre are very difficult to develop. Some authors have suggested improvements for some of these problems, but they all faced major limitations [2-6].

Because of these drawbacks, 3D-finite element analysis (FEA) of SCFs is rapidly gaining attention. This technique allows an accurate determination of SCFs without major assumptions. The FEA results can be used as input for strength models [7, 8].

Several authors noticed significant discrepancy between experimental and modelled tensile behaviour [9, 10]. Batdorf et al. [9] indicated the variation in fibre spacing as the major cause for this discrepancy. Incorporation of a random 1D fibre packing led to a smaller discrepancy between experiment and model. However, the results of Hedgepeth et al. [11, 12] clearly showed a significant difference between 1D and 2D fibre packings.

2 Materials and methods

This paper analyses the stress concentrations around a broken fibre in unidirectional composites with a random fibre packing. There are three distinct steps in creating these models: (1) generation of the random fibre packing, (2) creation of the FE model, and (3) extraction of the data.

The random fibre packing generator is based on the generator developed by Melro et al. The generator requires three input parameters: the fibre radius, the fibre volume fraction and the size of the representative volume element (RVE). The first step is a hard-core algorithm, which puts fibres at random coordinates within a square RVE. This step avoids overlapping between fibres but is limited to a fibre volume fraction of about 50%. The second step tries to move each fibre closer to its nearest, second nearest or third nearest neighbour. The third and final step pushes the fibres on the edges of the RVE inwards. These 3 steps are repeated until the required fibre volume fraction is achieved. A full description can be found in [13]. We merely added a criterion for the minimal fibre distance. Instead of a minimal distance between the fibre centres of 2 times the fibre radius, we used a criterion which varies the minimal distance between 2 and 2,1 times the fibre radius. This minimal distance is randomly generated within that interval. This adaptation increases the statistical randomness.

The second step is the creation of the FE model. A circular model is created out the square RVE of the random fibre packing generator. In contrast with hexagonal or square packing models [7, 14], a random packing model cannot be reduced due to lack of symmetry and the full 360° model had to be used. Even for the square and hexagonal packings, the 360° model was deliberately chosen to avoid any influence on the results. The applied boundary conditions are shown in figure b. A vertical displacement is applied to the entire top surface, which equals a strain of 0,1%. Symmetry in the fibre direction is applied to the bottom surface, except for the broken fibre. These boundary conditions have been used previously to represent a unidirectional composite with one broken fibre in the middle [7]. The mesh is refined on the bottom surface and near the broken fibre, as can be seen respectively in figure 1c and d.

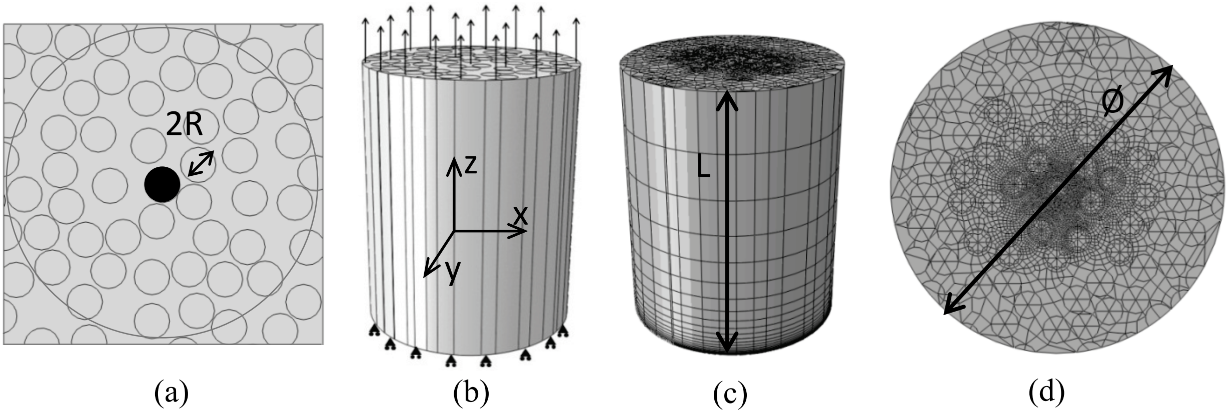

Figure 1. Description of the model (a) Creation of a circular model out of the square RVE (b) boundary conditions (c) mesh in a side view (d) mesh in top view.

Length L (see figure 1c)	40*R
Diameter Ø (see figure 1d)	24*R
Number of elements	> 180000 elements
Type of elements	70-90% second-order brick elements 10-30% second-order wedge elements
Matrix	Epoxy: isotropic, Young's modulus = 3 GPa, Poisson's ratio = 0,4
Fibre	Glass fibre: isotropic, Young's modulus = 70 GPa, Poisson's ratio = 0,22

Table 1. Parameters of the FE model

The stress field is obtained in Abaqus. In the third step, the necessary data is extracted out of the stress field. Within each fibre, imaginary planes are created on which the average stress is calculated. In each plane, the longitudinal fibre stress is probed in at least 2400 locations and averaged out over the plane. An example of this average stress as a function of the distance along the broken fibre is shown in figure 2. Three important parameters are calculated. In accordance with Rosen's definition [15], the ineffective length is defined as the location at which 90% of the stress is recovered in the broken fibre (see figure 2a). The stress concentration factor (SCF) at a certain z-coordinate $z*$ is calculated as the relative increase in fibre stress σ at that point divided by the fibre stress σ far away from the failure location (see equation 1) [1]:

$$SCF(z = z*) = \frac{\sigma(z = z*) - \sigma(z = \infty)}{\sigma(z = \infty)}.100\% \tag{1}$$

where z is the z-coordinate, $z*$ is the z-coordinate where the stress is evaluated, and σ is the longitudinal fibre stress.

In line with the ineffective length for the broken fibre, the overload length is defined for the intact fibres. This parameter is defined as the distance from the crack plane at which the fibre has a SCF of 0% (see figure 2b).

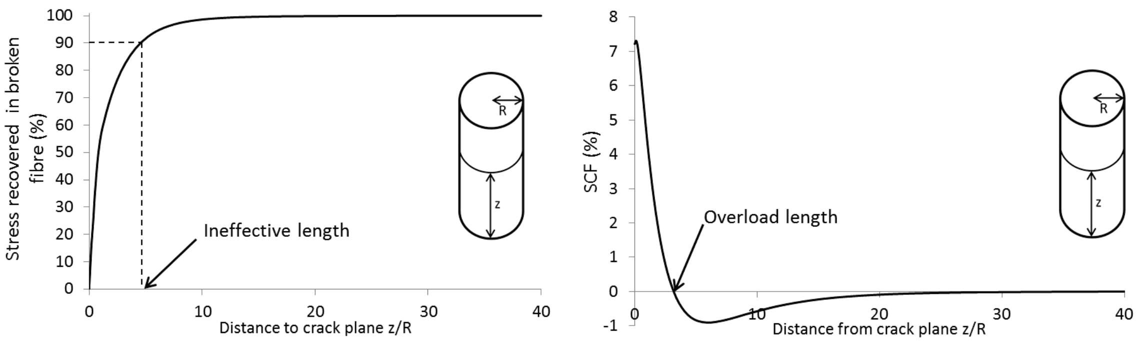

Figure 2. Illustration of the definitions for (a) ineffective length and (b) overload length.

3 Results

3.1 Fibre packing

This section examines the fibre packing. Two non-random fibre packings, namely square and hexagonal, are compared to 6 random fibre packings. The glass fibre volume fraction is 70%. The results are shown in figure 3.

The ineffective lengths are larger for hexagonal than for random packings. Square packings have intermediate values (see figure 3a). For hexagonal packings, the distance from the broken fibre to the nearest neighbour is larger than for square or random packings. This can be seen from the distance of each data point in figure 3b and c. Moreover, the main contribution to the stress recovery comes from material immediately surrounding the broken fibre. This means that the further away the fibres are from the broken fibre, the less they contribute to the stress recovery. This leads to a larger ineffective length.

Random fibre packings show much higher SCFs than structured packings, because smaller distances are possible. However, when looking at the same distance, the SCFs for the structured packings are slightly higher than for the random packings (see figure 3b). This is mainly valid at d/R values below 0,5. At larger distances, the difference fades out. In random fibre packings some fibres are very close to the broken fibre. These fibres carry a very high SCF and thus shield the other intact fibres. In hexagonal packings, 6 fibres are located at exactly the same distance. Consequently, none of these 6 fibres shield the other ones, which results in a higher SCF than in the random fibre packing.

Finally, the overload lengths for random fibre packings are significantly lower than those for structured packings, see figure 3c. This is related to the ineffective length, which is also smaller for random packings. If the ineffective length is smaller, the influence of the fibre breakage will also be spread out over a larger length. This results in a larger overload length.

Random fibre packings have a lower ineffective length, SCF and overload length than in the case of structured packings. The decrease of these three parameters decreases the probability of a second fibre breakage in the neighbourhood. Since current models mainly use hexagonal packings, random fibre packings would increase the gap between modelled and measured tensile strength. However, figure 3b shows a second effect which counteracts this conclusion. The random fibre packings have SCFs of up to 13%, while the highest SCF for hexagonal packings is only 5%. In order to know the combined influence on the strength, a full strength model for random fibre packings is needed.

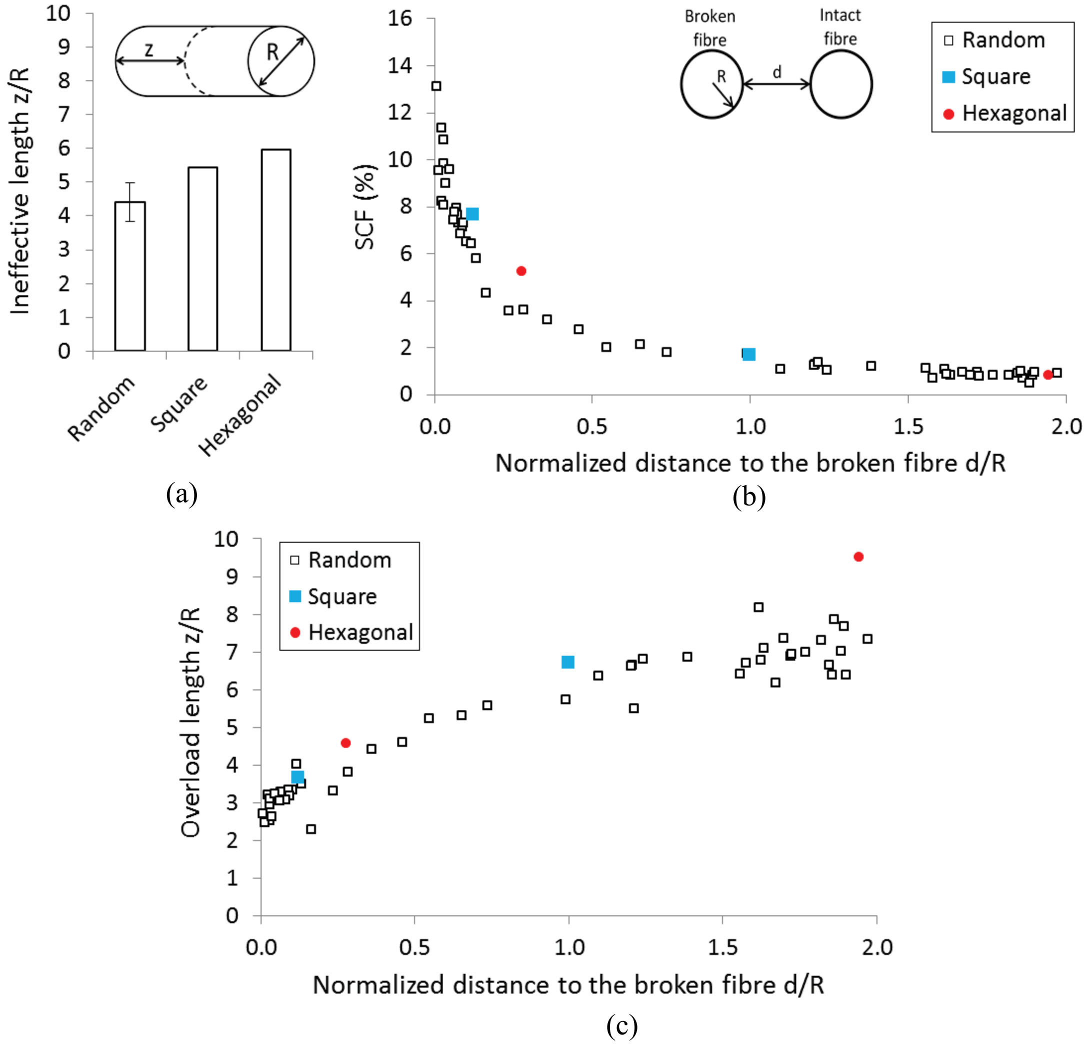

Figure 3. Comparison of random fibre packings versus square and hexagonal packings (a) ineffective length (b) SCF (b) overload length.

3.2 Fibre volume fraction

This section examines the influence of the fibre volume fraction. Three glass fibre volume fractions were examined: 30%, 50% and 70%. The results are shown in figure 4.

Figure 4a shows the decrease of the ineffective length with increasing fibre volume fraction. In the 70% case, 5-6 fibres are within a d/R of 1. This results in a high homogenized shear stiffness and thus a small ineffective length. The 30% case can have a 60% smaller ineffective length, because of the lower homogenized stiffness.

The fibre volume fraction also has a major effect on the SCF, see figure 4b. The SCF for the 70% case is less than half of the SCF in the 30% case for the same normalised distance. This is due to the shielding effect. Nearby, intact fibres shield the stress concentrations from the fibres which are further away. In the 70% case, more fibres are nearby, which yields a more pronounced shielding effect and a lower SCF at the same normalised distance. Literature states that the SCF increases with fibre volume fraction. At first sight, this is in contradiction with figure 4. However, these results were all obtained for square or hexagonal packings. In these structured packings, the distance from the broken fibre is directly linked with the fibre volume fraction. In random packings however, these two parameters are decoupled.

The overload length also shows a clear trend. A high fibre volume fraction results in a small overload length. This is again related to the ineffective length. When the ineffective length is small, the stress is recovered on a short length. This affects a smaller portion of the intact fibres and thus results in a smaller overload length.

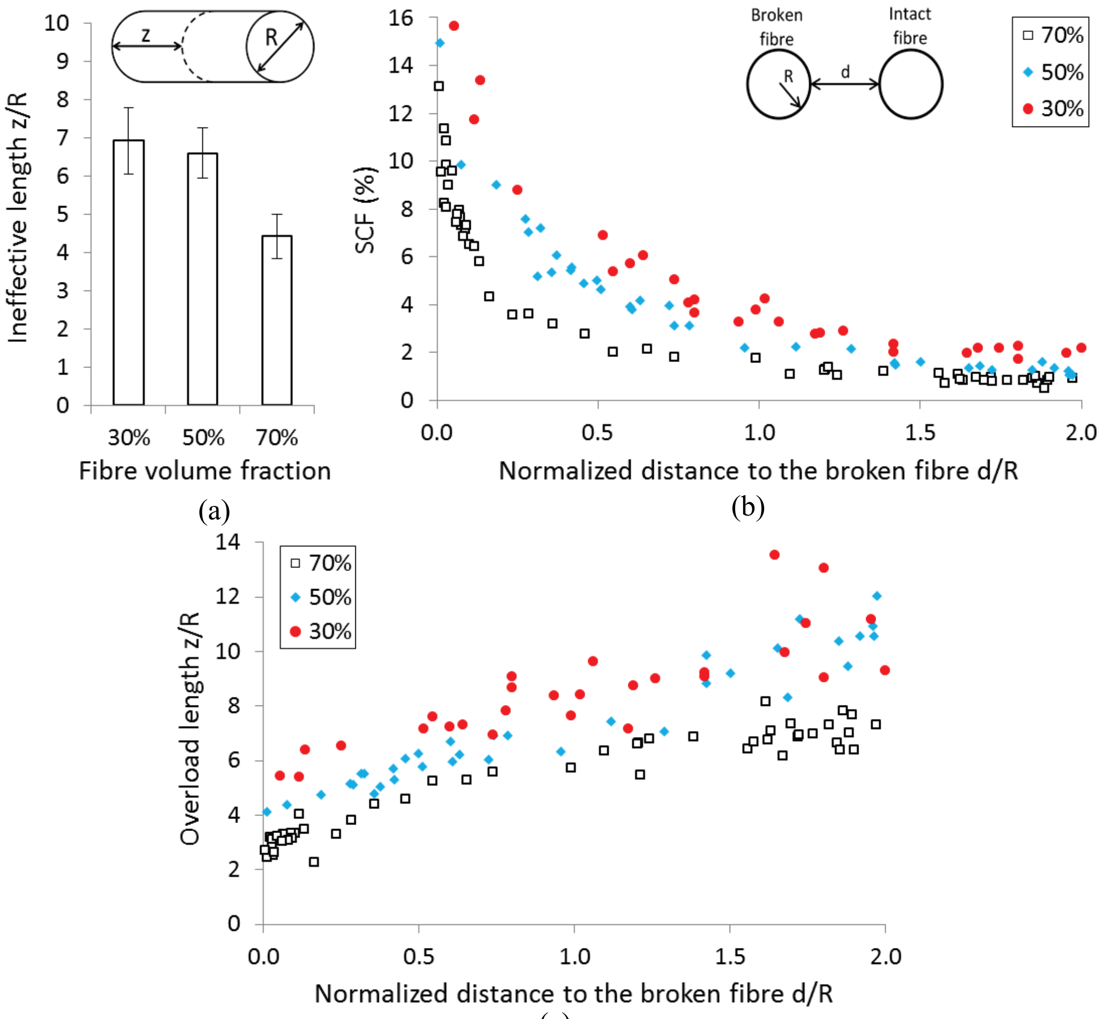

(a) (b) (c)

Figure 4. Comparison of random fibre packings for various fibre volume fractions: (a) ineffective length (b) SCF (c) overload length.

4 Conclusion

Random fibre packings behave significantly different from hexagonal and square packings. Compared to structured packings, random packings show a smaller ineffective length and, at the same distance, the SCF and overload length are smaller. However, apart from this first effect, the maximal SCF is also up to three times bigger for random packings. In contrast with the first effect, the second effect increases the failure probability of the intact fibres.

For random fibre packings, a higher fibre volume fraction results in smaller ineffective lengths and, at the same distance, in smaller SCFs and overload lengths. However, higher fibre volume fractions also have more fibres nearby the broken fibre and thus carrying a higher SCF. Therefore, the final effect on the failure probability of the intact fibres is unknown.

This paper has shown the importance of using random fibre packings for analysing stress concentrations. The next step is to develop a strength model which can incorporate random fibre packings. This model can analyse the influence of the fibre packing and volume fraction on the strength of unidirectional composites.

5 Acknowledgements

The work leading to this publication has received funding from the European Union Seventh Framework Programme (FP7/2007-2013) under the topic NMP-2009-2.5-1, as part of the project HIVOCOMP (grant agreement n° 246389). The authors thank the Agency for Innovation by Science and Technology in Flanders (IWT) for the grant of Y. Swolfs.

6 References

[1] Fukuda H. Stress concentration factors in unidirectional composites with random fiber spacing. *Composites Science and Technology*, **22**, pp. 153-163 (1985).

[2] Ochiai S., Hojo, M., Osamura, K. General expression of the shear lag analysis for unidirectional elastic fiber-elastic matrix composites. *Zeitschrift Fur Metallkunde*, **84**, pp. 796-801 (1993).

[3] Landis C.M., McMeeking, R.M. Stress concentrations in composites with interface sliding, matrix stiffness and uneven fiber spacing using shear lag theory. *International Journal of Solids and Structures*, **36**, pp. 4333-4361 (1999).

[4] Zeng Q.D., Wang, Z.L., Ling, L. A study of the influence of interfacial damage on stress concentrations in unidirectional composites. *Composites Science and Technology*, **57**, pp. 129-135 (1997).

[5] Okabe T., Takeda, N., Kamoshida, Y., Shimizu, M., Curtin, W.A. A 3D shear-lag model considering micro-damage and statistical strength prediction of unidirectional fiber-reinforced composites. *Composites Science and Technology*, **61**, pp. 1773-1787 (2001).

[6] Beyerlein I.J., Landis, C.M. Shear-lag model for failure simulations of unidirectional fiber composites including matrix stiffness. *Mechanics of Materials*, **31**, pp. 331-350 (1999).

[7] Xia Z., Curtin, W.A., Peters, P.W.M. Multiscale modeling of failure in metal matrix composites. *Acta Materialia*, **49**, pp. 273-287 (2001).

[8] Okabe T., Ishii, K., Nishikawa, M., Takeda, N. Prediction of Tensile Strength of Unidirectional CFRP Composites. *Advanced Composite Materials*, **19**, pp. 229-241 (2010).

[9] Batdorf S.B., Ghaffarian, R. Size effect and strength variability of unidirectional composites. *International Journal of Fracture*, **26**, pp. 113-123 (1984).

[10] Curtin W.A., Takeda, N. Tensile strength of fiber-reinforced composites: II. Application to polymer matrix composites. *Journal of Composite Materials*, **32**, pp. 2060-2081 (1998).
[11] Hedgepeth J.M. Stress concentrations in filamentary structures. *NASA TN*, **D-882**, pp. 1-36 (1961).
[12] Hedgepeth J.M., Van Dyke, P. Local stress concentrations in imperfect filamentary composite materials. *Journal of Composite Materials*, **1**, pp. 294-309 (1967).
[13] Melro A.R., Camanho, P.P., Pinho, S.T. Generation of random distribution of fibres in long-fibre reinforced composites. *Composites Science and Technology*, **68**, pp. 2092-2102 (2008).
[14] Nedele M.R., Wisnom, M.R. Three-dimensional finite element analysis of the stress concentration at a single fibre break. *Composites Science and Technology*, **51**, pp. 517-524 (1994).
[15] Rosen B.W. Tensile failure of fibrous composites. *Aiaa Journal*, **2**, pp. 1985-1991 (1964).